15B.4

DEVELOPMENT OF NOWCASTING METHOD BASED ON SPATIAL SCALE ANALYSIS OF PRECIPITATION DISTRIBUTION OBSERVED BY X-BAND POLARIMETRIC RADAR

Nozomu TAKADA*, Shuichi IKEBUCHI
Meteorological Engineering Center, Inc., Japan

Yuusuke TANAKA,
Japan Agency for Marine-Earth Science and Technology, Japan

Eiichi NAKAKITA
Disaster Prevention Research Institute Kyoto University, Japan

1. INTRODUCTION

Recently, there are numbers of disasters caused by localized heavy rainfall in urban areas in Japan. To watch these localized heavy rainfall, Ministry of Land, Infrastructure, Transport and Tourism (MLIT) provides X-band polarimetric (multi parameter) RAdar Information Network (XRAIN) data experimentally from 2010. Specifications of XRAIN data are as follows. Spatial resolution is 250m and time resolution is 1minute. As for operational C-band radars operated by MLIT, spatial resolution is 1km, and time interval is 5minutes. Thus, XRAIN has advantages over conventional C-band radars. Furthermore, XRAIN data have higher quality in point that multi-parameter data, such as KDP and ZDR, can be used in estimating rainfall intensity. Comparison of the above two radars is shown in Table.1.

* *Corresponding author address*: Nozomu Takada
Meteorological Engineering Center, Inc.
1-8-5, Kyomachibori, Nishi-ku, Osaka Japan
e-mail: n.takada@meci.jp

As shown in Table.2, rainfall phenomena are classified to convective and stratiform. Localized heavy rainfall, which belongs to convective phenomenon, has small spatial scale and short time scale.

For investigating characteristics of localized heavy rainfall, XRAIN data with high resolution in space and time has an advantage to data observed by conventional C-band radar.

Rainfall prediction data with high accuracy become necessary for disaster prevention as well as observed data. Especially in urban area in Japan, prediction until 1 hour ahead is considered to be useful for evacuation.

Table.1 Comparison of radar specification in Japan

Item \ Radar	XRAIN	Conventional C-band Radar Network
Grid Interval	250 m	1 km
Time Resolution	1 min.	5 min.
Observed element	$Z, ZDR, KDP, \rho hv$	Z

Table.2 Characteristics of convective and stratiform precipitation

	Convective	Stratiform
Example of phenomena	Localized heavy rainfall	Stationary front, low pressure
Spatial scale	Less than about 30 km	Larger than about 100 km
Time scale	Few 10 minutes – few hours	Longer than few hours
Rainfall intensity	Strong (sometimes larger than 100mm/hour)	Weak (less than 20 mm/hour)
Movement of precipitation distribution	Mainly moved by wind between 3 - 5(km), and affected by wind lower than 1 (km)	Mainly moved by wind between 3 - 5(km)

Though accuracy of meso-scale meteorological model has improved, nowcasting method with radar data is more effective until 1 hour ahead. However, it is still difficult to predict accurately localized heavy rainfall even by nowcasting method, because of the different characteristics of movement between convective and srtariform.

Methods to extract convective precipitation distribution have been developed paying attention to the difference of rainfall intensity (Yoshida et al. 2012, Johnson et al. 1998, Handwerker 2002). However, it is difficult to extract convective precipitation during developing stage through these methods, and that leads to prediction with low accuracy.

In this study, we have developed a new nowcasting method to improve accuracy of prediction for localized heavy rainfall, considering the difference of spatial characteristics between convective and stratiform. In order to separate convective precipitation from total precipitation distribution, wavelet transform method is used. An example of separation of precipitation through wavelet transform is shown in Fig.1. Separated precipitation distributions are predicted respectively by adequate method for each distribution, and then two distributions, namely convective and stratiform are merged to gain total precipitation distribution. Flow of developed nowcasting method is shown in Fig.2.

In this study, a method to extract convective precipitation distribution is described in chapter 2, and the prediction method considering characteristics of convective and stratiform precipitation is described in chapter 3. In chapter 4, outline of the prediction method considering growth and decay of convective cells are described. Predicted results by the above methods are also shown. Conclusion and future tasks are shown in chapter 5.

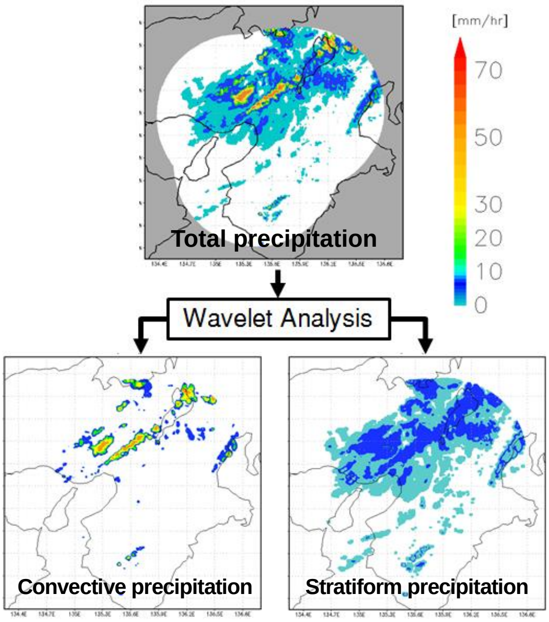

Fig.1 An example of separation of precipitation distribution by wavelet analysis

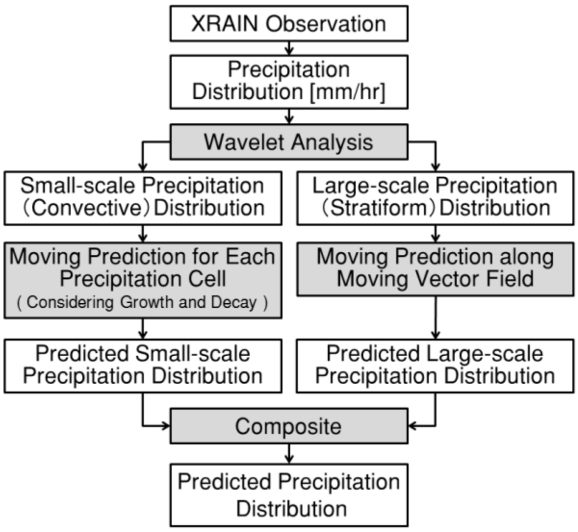

Fig.2 Flow of developed nowcasting method

2. DEVELOPMENT OF A METHOD TO EXTRACT CONVECTIVE PRECIPITATION

2.1 A METHOD TO SEPARATE PRECIPITATION DISTRIBUTION

Turbulence phenomena were analyzed by two dimensional wavelet transformation (Fage 1992). High-pass filtering method was used for the results of wavelet analysis (Torrence and Compo 1998). The above methods are applied to extract convective precipitation in this study.

Considering the time required for calculation and wave number distribution of target phenomena, Real Mexican Hat function is used as wavelet function. Length scale used for the translation S_n (n = 1 , $n_{\max}$,here, $n_{\max}$ is the number of analysis data) is defined as follows.

$$S_n = S_{\min} \times 2^{(n-1)\Delta j} \qquad \text{Eq.(1)}$$

$S_{\min}$ is minimum analyzable length, which is equal to double of grid size of observation data, and Δj is interval of length scale presented by exponential function.

In this study, length scale S_c , which is correspond to maximum length of convective precipitation distribution is set, and scales shorter than S_c is used to gain convective precipitation distribution by inverse wavelet transformation (high-pass filtering). The convective precipitation distribution gained by the method is defined as "small-scale precipitation distribution"(SPD). The distribution, where SPD is subtracted from original distribution is defined as "large-scale precipitation distribution"(LPD), which is considered to be stratiform precipitation distribution.

2.2 APPLICATION TO XRAIN DATA

A method to extract convective precipitation distribution is applied to XRAIN data. Time resolution and update interval of XRAIN data is 1 minute, and spatial grid size is 7.5" in latitude and 11.25" in longitude. Spatial resolution of XRAIN data is about 250 m. Analysis area is set to 33.50°N to 35.75°N in latitude and 135.25°E to 137.00°E in longitude. The number of grid from west to east is 880 and that of south to north is 1080.

XRAIN data of analysis area is assumed to be in regular interval of 250 m, and the extracting method of convective precipitation distribution described in 2.1 is applied. Minimum analysis scale $S_{\min}$ is 500 m. Considering characteristics of meso-beta phenomena and the time required for calculation, S_c is set to 16km and Δj is set to 0.25. The result of extraction of convective precipitation distribution of 2011.6.10 19:20(JST) is shown in Fig.3. As shown in Fig.3, convective precipitation distribution is extracted from XRAIN data distribution as small-scale distribution.

In small scale precipitation distribution, area surrounded by isoline of precipitation intensity of p_c is defined as "precipitation cell". A "precipitation cell" contains precipitation belong to single cumulonimbus cloud or clouds organized in a line by some cumulonimbus clouds. In this study, p_c is set to 2 mm/hour.

3. DEVELOPMENT OF PREDICTION METHOD

3.1 OUTLINE OF PREDICTION METHOD

Considering characteristics of convective and stratiform precipitation, SPD and LPD are moved respectively. SPD is predicted as follows. Precipitation cell of different time is identified, and each cell in SPD of initial time is moved by vector calculated for each cell respectively. LPD is predicted along moving vector field. Predicted SPD and LPD are merged to gain the final predicted precipitation distribution.

1) A METHOD TO TRACK CELLS

A precipitation cell in a SPD is related to cell(s) of different time. The identification is determined by maximizing correlation coefficient. When a cell of past time is related to cells of current time, the cell is considered to be divided. When a cell of current time is related to cells of past time, the cells are considered to be combined. When no cell in past is related to a cell of current time, that is, maximum correlation coefficient is less than 0.5, the current cell is considered to be generated.

2) ESTIMATION OF MOVING VECTOR OF SPD

TREC method (Rinehart 1979) is used to identify moving vector of each precipitation cell in SPD. SPD of initial time, that of 2 minutes past, and 4 minutes past are used for the identification.

3) ESTIMATION OF MOVING VECTOR OF LPD

To identify the moving vector field of large scale precipitation distribution, analysis area is divided to $m_{sec} \times n_{sec}$ areas. For each divided area, moving vector is identified to minimize R.M.S.E. by TRED method (Laroche and Zawadzki 1995). The vector is assumed to be moving vector of the center of the area, and vector of every observation point is determined by linear interpolation. LPD of initial time, that of 6 minutes past and 12 minutes past are used for the identification.

4) PREDICTION METHOD OF LPD

Semi-Lagrange backward method (Germann and Zawadzki) is used to predict LPD. In this method, a predicted precipitation at a grid point is determined as the value of the grid tracking back along moving vector field.

3.2 PREDICTION USED BY XRAIN DATA

Developed prediction method described in 3.1 is applied to rainfall events observed by XRAIN. The divide numbers to identify large scale moving vector, m_{sec} and n_{sec} is set to 2.

Fig.3 shows precipitation distribution at prediction initial time. Fig.4 shows observed and predicted precipitation distribution of 10 and 30 minutes after prediction initial time. Accuracy of predicted result is evaluated in comparison of conventional prediction method, which predicts without extracting convective precipitation distribution. In Fig.4, results by conventional method (abbreviated as CONV) are shown in (b) and (f), and results by developed method (abbreviated as SPRT) are shown in (c) and (g).

Fig.5 shows time series of observed and predicted rainfall intensity at the black round point shown in Fig.3(a). Heavy rainfall intensity around 30 minutes is well predicted by SPRT, which can't be predicted by CONV.

Fig.6 shows time series of R.M.S.E. of predicted precipitation distribution to observed distribution calculated in black square frame shown in Fig.3(a). Compared to CONV(black line), SPRT(blue line) shows good accuracy during 0-60 minutes lead time. The advantage of CONV becomes larger as lead time become longer.

By separating precipitation distribution to small-scale and large-scale distributions and moving the distributions respectively, accuracy of nowcasting has improved.

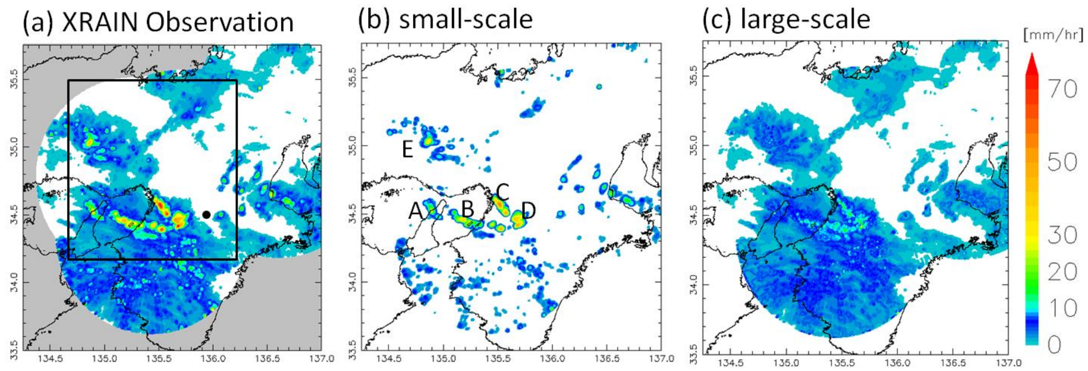

Fig.3 An example of extraction of convective precipitation (2011.6.10 19:20).
(a)XRAIN radar observation (b)Small-scale (correspond to convective precipitation) (c)Large-scale (correspond to stratiform precipitation) Black square frame in (a) shows R.M.S.E. analysis area.(34.2-35.5°N , 134.7-136.2°E)

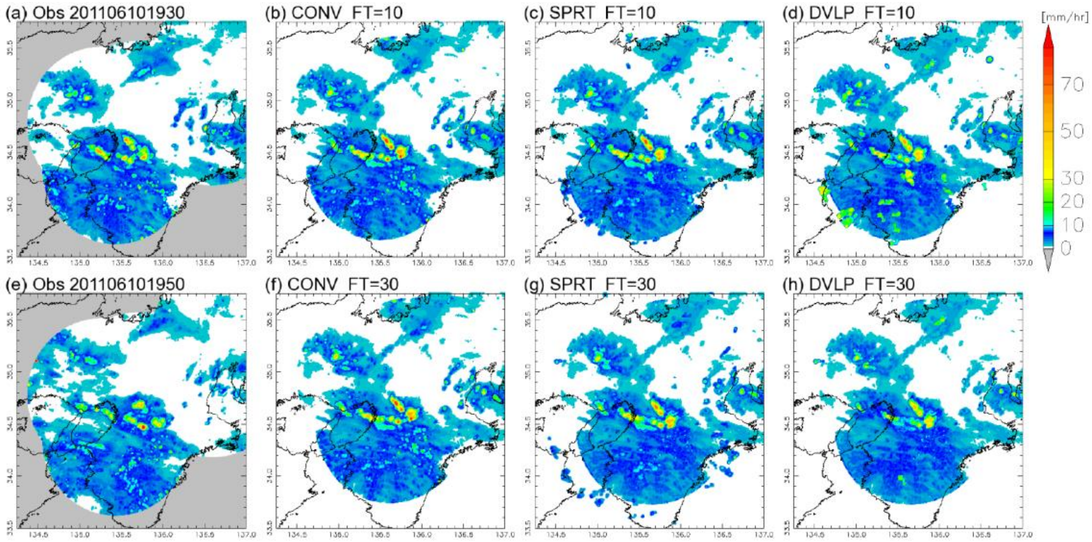

Fig.4 Examples of prediction results.(Initial time: 2011.6.10 19:20) Upper:10 minutes after initial time. Lower: 30minutes after initial time. (a,e):XRAIN observation (b,f):Conventional method (c,g):Developed method considering difference of moving vector (d,h):Developed method considering growth and decay of convective cells

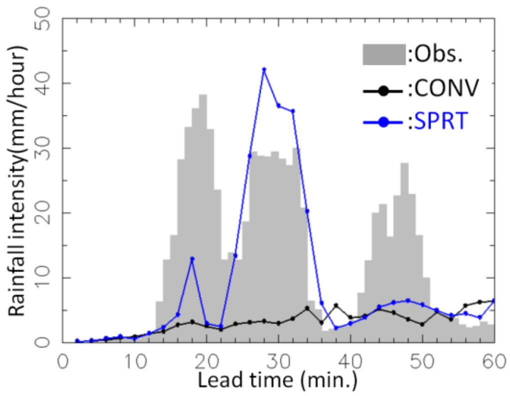

Fig.5 Time series of rainfall intensity at the black round point in Fig.3 (a) (34.48°N 135.93°E) (2011.6.10 19:20 - 20:20)

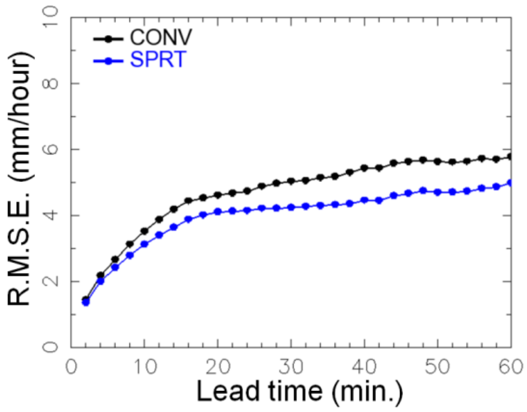

Fig.6 R.M.S.E. of predicted precipitation in black square frame in Fig.3(a) (2011.6.10 19:20 – 20:20)

4. DEVELOPMENT OF PRECIPITATION PREDICTION METHOD CONSIDERING GROWTH AND DECAY OF CONVECTIVE CELLS

4.1 CHARACTERISTICS OF GROWTH AND DECAY OF CONVECTIVE CELLS

To put growth and decay process of convective precipitation into nowcasiting model, time evolution characteristics of convective precipitation are investigated. Area of precipitation cell (A [km^2]), total precipitation in a cell at an instant (V [m^3/hour]), maximum precipitation intensity in a cell (P_{max} [mm/hour]) and averaged rainfall intensity ($P_{ave} = V / A \times 10^{-3}$ [mm/hour]) are selected as quantities to investigate, because they are considered to be important quantities to evaluate time evolution of precipitation. Relationships between the quantities and time evolution of them are investigated. SPD distributions extracted by the method described in chapter 2 are used in the analysis.

Fig.7(a) shows the relationship between

$\log_{10}(A)$ and $\log_{10}(V)$. Fig.7(b) shows the relationship between P_{ave}, and $P_{\max}$ during 2012.7.30 - 20:30(JST). During the period, heavy precipitation occurred in the analysis area (Kinki Region in Japan), and selected quantities of every 1 minute during the period are plotted in Fig.7(a)(b).

From Fig.7(a)(b), the relationship between A and V, and P_{ave} and $P_{\max}$ are approximated as follows.

$$V = cA^p \qquad \text{Eq.(2)}$$

$$P_{\max} = aP_{ave} + b \qquad \text{Eq.(3)}$$

Table.3 shows identified value of a, p, c, b for including other 2 events. These parameters are identified to be nearly equal value in 3 events.

If V (or A) is predicted, A (or V) is calculated from Eq.(2), and $P_{\max}$ is calculated from Eq.(3). Characteristics on time evolution of V are investigated. Precipitation cells which didn't combine nor separate are picked up and analyzed. Fig.8 shows time series of total precipitation in a cell during 2012.7/30 12:00 - 20:30. In Fig.8, time after cell generation is shown as $\hat{t}$ which is normalized by cell life time, and total precipitation in a cell is shown as $\hat{V}$ which is normalized by total precipitation provided by the cell during its life time. Values calculated by Eq. (4) are shown by red line in Fig.8. Fig.8 shows that time evolution of $\hat{V}$ is well presented by Eq.(4).

$$\hat{V} = 6\hat{t}(\hat{t} - 1) \qquad \hat{t} \in [0,1] \qquad \text{Eq.(4)}$$

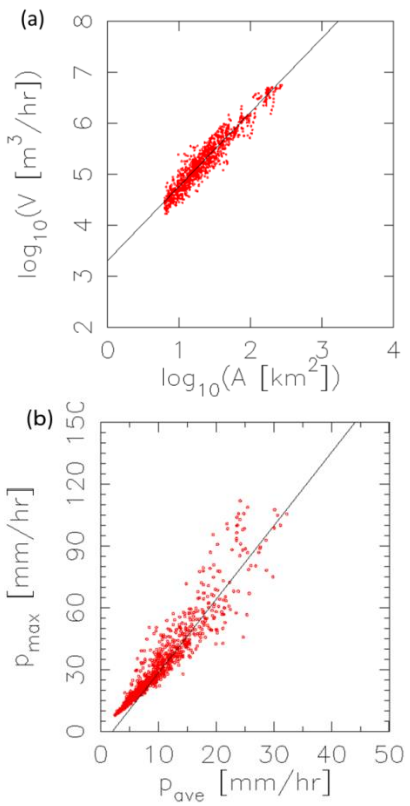

Fig.7 Relationships between selected quantities. (2012.7.30 12:00 - 20:30)
(a) $\log_{10}(A)$ and $\log_{10}(V)$
(b) P_{ave} and $P_{\max}$

Table.3 Coefficients of Eq.(2) and Eq.(3)

Analysis Period	$V = cA^p$		$P_{\max} = aP_{ave} + b$	
	$c[\times 10^2]$	p	a	b
2012.7.30 12:00 - 20:30	1.99	1.46	3.57	-7.44
2010.8.13 21:00 - 8.14 22:00	2.07	1.40	3.51	-7.60
2010.8.25 12:00 - 17:30	2.14	1.45	3.58	-7.89

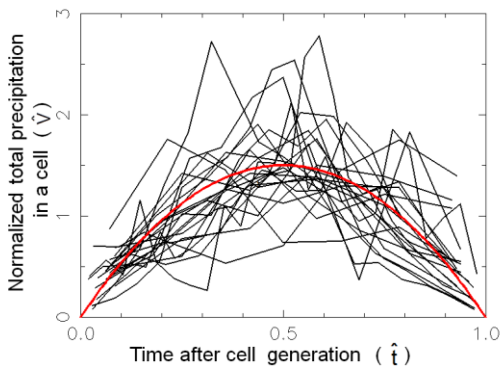

Fig.8. Time series of normalized total precipitation in a cell. Cells which didn't combine nor separate are plotted. (2012.7.30 12:00 - 20:30)

4.2 PREDICTION METHOD

Based on the results of 4.1, prediction method considering growth and decay of precipitation cell are as follows.

First, life stages of precipitation cells are estimated as follows. Life stage of a cell is categorized to 4 stages. They are developing (stage-1), mature stage (stage-2), decaying stage (stage-3), and re-developing stage (stage-4). Stage of a cell is identified as follows. Cells of $\hat{t} \in [0,0.4]$ are classified to stage-1, cells $\hat{t} \in [0.4,0.6]$ are classified to stage-2, and cells $\hat{t} \in [0.6,1]$ are classified to stage-3. If a cell passes through stage-3 and develops again, the cell is classified to stage-4, and cells of stage-4 is treated same as those of stage-1.

Next, Eq.(4) is adopted for each cell according to the classification of life stage. A cell of stage-1 or stage-4 is assumed to be $\hat{t}_{now} = 0.2$, that of stage-2 is assumed to be $\hat{t}_{now} = 0.5$, and that of stage-3 is assumed to be $\hat{t}_{now} = 0.6$. Left life time of a cell can be calculated by the equation $T = t_{now} / \hat{t}_{now}$, here $\hat{t}_{now}$ is time after the cell generation. Assuming that total precipitation of a cell at prediction initial time is V_{now}, total precipitation of the cell at t minutes, $V_f(t)$ .is gained by Eq.(5).

$$V_f(t) = 6V_{now}(\hat{t} + t/T)((\hat{t}_{now} + t/T) - 1) \qquad \text{Eq.(5)}$$

By using $V_f(t)$ calculated in Eq.(5) and Eq.(3) and coefficients value $c = 2000$, $p = 1.4$, $a = 3.5$,and $b = 7$ determined from Table.3, area of a cell and maximum rainfall intensity in the cell are calculated. By applying the method to all precipitation cells in small scale distribution, precipitation distribution of small-scale is predicted.

4.3 APPLIED EXAMPLE

Fig.4(d) and (h) show precipitation distributions predicted by the method including precipitation growth and decay (abbreviated as DVLP) for 10 and 30 minutes after initial time.

Fig.9 shows time series of predicted rainfall intensity at the round black point in Fig.3 (a).

Fig.10 shows time series of R.M.S.E. of each prediction model. Fig.9 shows that DVLP predicts better than SPRT for heavy precipitation of 25-35minutes after initial time. Fig.10 shows that DVLP has higher accuracy (low R.M.S.E.) than SPRT after 16 minutes.

As described above, considering growth and decay of convective rain clouds has improved accuracy of nowcasting method. The developed time evolution model is very simple at present, and so there are some points to be improved. By investigating other heavy rainfall events, and improving prediction method based on the analysis, the accuracy of the prediction model is considered to be improved.

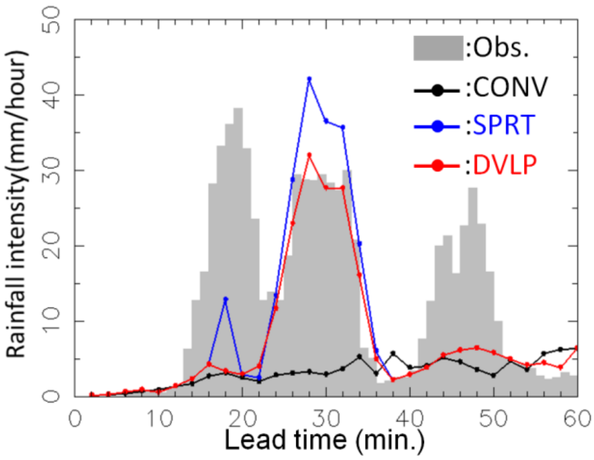

Fig.9 Time series of rainfall intensity at filled circle in Fig.3 (a) (2011.6.10 19:20 - 20:20)

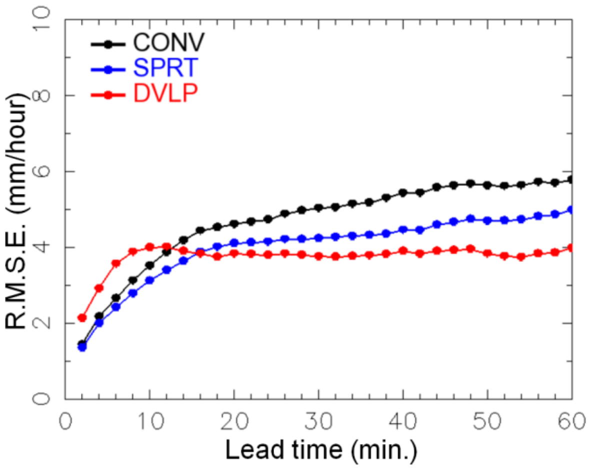

Fig.10 R.M.S.E. of predicted precipitation in frame in Fig.3(a) (2011.6.10 19:20 – 20:20)

5. CONCLUSION

We have developed a new nowcasting method utilizing XRAIN data in order to improve accuracy of prediction for localized heavy rainfall. The method to extract convective precipitation distribution from total precipitation distribution has been developed through wavelet transform. By the method developed in this study, precipitation distribution is separated to convective and stratiform distribution. The distributions are predicted respectively by adequate moving method for each distribution, and then they are composited to gain final predicted precipitation distribution. The results of developed model showed better agreement with observed data than the results of conventional method in which no spatial separation of precipitation distribution is considered.

The extracted convective precipitation distributions are analyzed and characteristics of convective rain clouds are investigated. Based on the analysis, we have developed a simple model including growth and decay process of rain clouds. The developed model has higher accuracy than the model without considering growth and decay process for the prediction after lead time of 16 minutes.

By investigating other heavy rainfall events and improving prediction method based on the analysis, the accuracy of the prediction model is considered to be improved.

Acknowledgements

XRAIN data used in this study is provided by “Technical Development Consortium of X-band Polarimetric Radar” of MLIT. The authors thank MLIT Japan.

References

Farge, M.: Wavelet transforms and their applications to turbulence,*Ann. Rev. Fluid Mech.*, Vol.24, pp.395-457, 1992.

Germann, U. and Zawadzki, I.: Scale-dependence of predictability of precipitation from continental radar images. PartI: Description of the methodology, *Mon. Wea. Rev.*, Vol.130, pp.2859-2873, 2002

Handwerker, J.: Cell tracking with TRACE3D–a new algorithm,*Atmos. Res.*, Vol.61, pp.15-34, 2002.

Johnson, J. T., Mackeen, P. L., Witt, A., Mitchell, E. D.,Stumpf, G. J., Eilts, M. D. and Thomas, K.W.: The storm cell identification and tracking algorithm: An enhanced WSR-88D algorithm, *Wea. Forecasting*, Vol.13, pp. 263-276, 1998.

Laroche, S. and Zawadzki, I.: Retrievals of horizontal winds from single-Doppler clear-air data by methods of cross correlation and variational analysis, *J. Atmos. Oceanic Technol.*,Vol.12, pp.721-738, 1995.

Rinehart, R. E.: Internal storm motions from a single non-Doppler weather radar,NCAR/TV-146+STR, 1979.

Torrence, C. and Compo, G. P.: A practical guide to wavelet analysis, *Bull. Amer. Meteor. Soc.*, Vol.79, pp.61-78, 1998.

Yoshida S., R. Misumi, S. Shimizu, T. Maesaka, K. Iwanami and M. Maki, 2012: Validation of short-term forecasting of meso-γ scale convective systems based on a cell-tracking system, *SOLA*, 8, 141-144